## Project3 – Narrow-band Imaging of Nearby Galaxies

## Ludvig Doeser<sup>1</sup>

<sup>1</sup>Department of Astronomy, The University of Texas at Austin, Austin, TX 78712, USA

## 1. PURPOSE & EQUIPMENT

The 30 inch telescope at McDonald's Observatory in Fort Davis, Texas, will be operated remotely; it is equipped with the SDSS (Sloan Digital Sky Survey) filters ugri, plus a narrow-band filter centered on the Halpha spectral line (Balmer series, n=3-2transition). For the purposes of this observation of identifying star forming regions of nearby galaxies, the narrow-band filter will be the one of most interest. The broadband-filters g and r will also be used.

Problem Formulation—Obtain images of nearby bright galaxies in the H-alpha narrow-band filter, and the g and r-band broadband filters. The goal will be to identify star-forming regions as those which have knots of excess H-alpha emission (we observe in the broad-band as well so we can assess the continuum level across the galaxy). After flux-calibrating the galaxy image using field stars, use aperture photometry to measure the fluxes of these H-alpha knots, converting to the H-alpha luminosity using the known distances to these well studied galaxies. Finally, make a plot of the H-alpha luminosity function of HII regions, which is the distribution of the number of HII regions with a given H-alpha luminosity, pergalaxy, per dex of luminosity (units of number, per galaxy, per dex). Do this for a minimum of five galaxies.

## 2. OBSERVATIONS

## 2.1. 2020-04-19 — M81 & M51

Due to the different filter sensitivities it was recommended to take 5-15 minute exposures in the broadband-filters, and 20-30 minute exposures in the narrowband-filter.

Therefore, the original plan looked like:

Target	g [min]	r [min]	Ha [min]	Total time [hours]
M81	10	10	2x15	$\sim 1$
M51	12	12	2x16	~ 1
M101	12	12	2x16	~ 1

**Table 1.** Observation Plan developed before observing. In total, 12 frames were expected to be taken during 3 hours of effective observing (not including set-up and focusing etc).

At 1:31 UTC (20:31 local Fort Davis, Texas, time) we opened the dome, changed to the g-filter and used HIP47356 for focusing. We then took a 5 min long test exposure of M81 and decided, due to the low photon count, to take 12 minute exposures instead of 10. We decided to change the r-filter's exp.time accordingly.

Despite the plan to go for two consecutive 15 min exposures in the narrow-band, we ended up taking a single 30 min exposure. The reasoning was that the previous two images came out very nice and the only potential problems we saw with a long exposure were *losing track* of target and having to manually move the dome; however, by just clicking track in X0bs we would ensure that we wouldn't loose track, and by moving the dome around 5-7°ahead of the target in Azimuth we would ensure that the dome wouldn't pose a problem (as M81 had an altitude around 70°and moved quite slowly). We got the 30 min exposure and, of course, something was wrong, or at least that's what we suspected.

The image looked saturated in the middle and the spiral arms were not that visible (which we would expect as they ought to be bright in the Ha-filter). This was a blessing in disguise as we got a clue that the filter wheel might have been misaligned. Maybe it was not in the u-g-r-i-Ha order that xterm told us, but rather in Ha-u-g-r-i. We therefore changed filter to u and took a 15 min long exposure. It ended up looking quite bright in the spiral arms of the galaxy, which we expected (although this would also be the case in the u-filter). In addition, we looked at our g-image again and the particle count looked quite low, as if it could have been taken in the u-filter. From hereon we therefore suspected, being 90% sure, that the filter was not in the right order and used the mappings

xterm	u	g	r	i	На
suspected	На	u	g	r	i

**Table 2.** Suspected misaligned filter-wheel. We expected that u was in reality Ha etc.

Not being 100%, however, we decided upon taking images in all filters, with the down that we ended up taking only one 15 minute exposure in the narrow-band, and 12 minute exposures in the broad-bands. We reasoned that

this hopefully would be enough for the narrow-band as it had become a very clear night, with the moon being down. Due to limited observation time available this was in any case the best we could do, and we had to let M101 go. We would only have time for 2 galaxies tonight. In the end we got the frames:

Target	g [min]	r [min]	i [min]	Ha [min]	u [min]
M81	12	12	12	30	15
M51	12	12	12	15	15

**Table 3.** Frames obtained in the *suspected* filters and the corresponding exposure times. We suspected that r,i,u would be the filters that we would need as these in fact would map according to:  $r \mapsto g$ ,  $i \mapsto r$  and  $u \mapsto Ha$ .

#### 2.2. Filter wheel was installed incorrectly

On May 4 it was discovered that the SDSS H-alpha filter never was installed at all; instead, in its place the z-filter had been inserted. This was discovered after trying to match the filters with PAN-STARRS data without luck. As a result, no H-alpha images at all were collected.

However, by realizing that the H-alpha emission is included in the r-band image we could procede with the project. Hence, the data we obtained is not presented correctly in Table 3; what we got was:

Target	r [min]	i [min]	z [min]	u [min]	g [min]
M81	12	12	12	30	15
M51	12	12	12	15	15

**Table 4.** The frames that in fact were collected due to z being in the position were H should have been. From hereon only r,i and g were used.

## 2.3. Data provided for NGC6946

Due to the loss of H-alpha-images in the observation, another galaxy – NGC6946 – was also used in the analysis. Data for this galaxy was taken both in r- and  $H\alpha$ -bands in 2018. Corresponding calibration frames were provided.

## 3. RESULTS

## 3.1. Calibrations

For the galaxies M51 and M81 the filters r,g and i were used for the analysis and for NGC6946 r and  $H\alpha$  were used.

First all images were calibrated by subtracting a master bias frame and then by dividing by corresponding (to match filters) master flat frames. For M51 and M81 the g and i filters were reprojected onto the r-image to align them. For NGC6946 we had several images per

filter (2 for r and 3 for  $H\alpha$ ). All of these were reprojected to the first r-image. Then, the r- and  $H\alpha$ -images were mean-combined respectively to obtain one stacked image per filter.

After resizing the data arrays to exclude overscan columns and using interpolate\_replace\_nans to replace nan-values, which either were present from the beginning or were introduced (most likely in the edges of the data) due to the reprojection, the background was subtracted from each image. This would ensure that the median values for the images would be around zero.

Next, calibration of the images were made by comparing to PANSTARRS-catalogues. First, however, identification of the sources in each background-subtracted image was carried out. For all of these the photometry was done using the package photutils. DAOStarFinder was used to produce a catalog of all sources with a full-width half maximum of approximately 4.0 and a threshold of 4 times the standard deviation for the corresponding filter-image in question. The fluxes and magnitudes for these sources were then found using the aperture\_photometry-function at all apertures specified by the function Circular Aperture, which in turn used the sources' positions from the generated catalog. The galaxies themselves were masked as individual stars would be hard to find inside the galaxy, as shown in Fig.1.

Then the matching was carried out using the Vizierfunction from the astroquery.vizier-package. All sources within 60 arcsseconds from the source positions from the photutils-catalogs were extracted with query\_region and the star with the minimum distance was taken as the comparison star with which the calibration would be perform. For M51 and M81 the magnitudes for the matched PANSTARRS-stars were extracted for the r-,g- and i-filters as to be able to match the observed instrumental magnitudes in these with the corresponding PANSTARRS-magnitudes in the same filter. For NGC6946 only the r-magnitude was extracted as both r and  $H\alpha$ , which is residing within the r-band, had to be compared to the r-magnitudes from PANSTARRS. The zeropoint values are shown in Tab. 5 and the zeropoint plots are shown in Appendix A; these

Galaxy	$zp_r$	$zp_g$	$zp_i$	$zp_{Ha}$
M51	28.61	28.06	28.50	-
M81	28.59	28.13	28.62	-
NGC6946	27.85	-	-	26.20

**Table 5.** Zeropoint values calculated for all filters using the corresponding background-subtracted data, which hasn't been normalized with the exposure time.

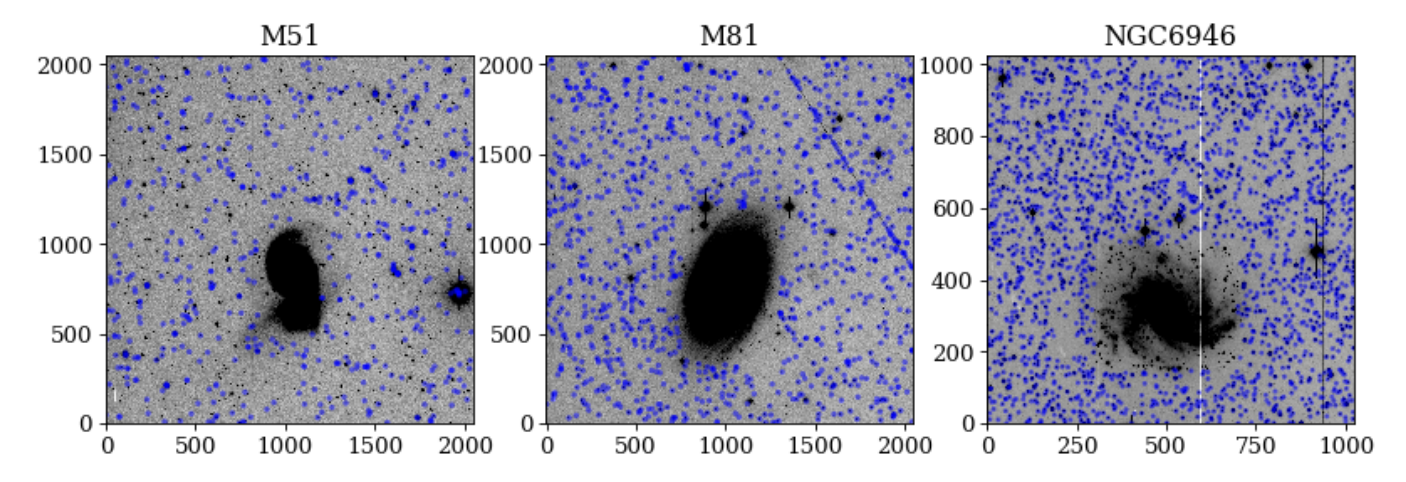


Figure 1. The observed data was photometrically calibrated using stars outside the galaxy regions; these were matched with data from PANSTARRS and calibration zeropoints were calculated to correct the observed data.

do all display a flat behaviour which was a feature that was used to determine what filters that were used during the observation. Non-flat zeropoint-curves namely mean that the observated instrumental magnitudes are matched with the magnitudes from a different filter from PANSTARRS.

The star-fluxes from all background-subtracted images in all filters, still excluding the galaxies, were calibrated according to

$$f_{\nu} = f \cdot 10^{-0.4 \cdot 48.6 - 0.4 \cdot zp},\tag{1}$$

where  $f_{\nu}$  is the flux in units of ergs/cm<sup>2</sup>/Hz, f is the initial flux in units of counts and zp the zeropoint. The magnitudes m were then calculated:

$$m = -2.5\log_{10}(f) - 48.6. (2)$$

The vast majority of the magnitudes, shown in Appendix B, are within the expected range of 16-19.

## 3.2. Finding HII-regions

To find regions bright in the Ha-filter two different methods were used due to the limited filters available. For M51 and M81  $method\ 1$  was used and for NGC6946  $method\ 2$  was used.

#### 3.2.1. Method 1 - M51 and M81

Only the images in the r-band and the i-band was used. Even though no image in the H-filter was taken, these regions could be extracted using the fact that this narrowband filter resides inside the r-band. First of all the background-subtracted images were reshaped to only display the galaxies. Then all pixel values from these images, which are in the units of counts, were converted to ergs/cm²/Hz using Eq. (1) with the corresponding zeropoints for r and i. The fluxes were in turn

converted to units of ergs/cm<sup>2</sup>/Å using

$$f_{\lambda} = f_{\nu} \frac{c}{\lambda^2},\tag{3}$$

where  $c=3\cdot 10^{18}$  is the speed of light in Å/s and  $\lambda$  is the corresponding filter's central wavelength, namely  $\lambda_r=6170$  Å and  $\lambda_i=7530$  Å. By subtracting the *i*-filter image from the *r*-filter a difference image was produced, see Fig. 2 for the result for M51 and Appendix C. The brighest areas, in black, in the difference im-

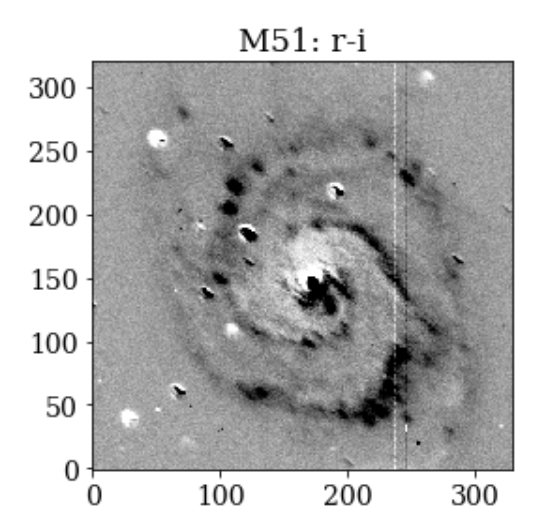


**Figure 2.** Difference image for M51 taken by subtracting the i-band from the r-band. The spiral arms seem to be host for bright Ha-regions.

age indicate Ha-regions. Before identification of these regions with DaoFind, however, we convolve the original background-subtracted images (still in  $\rm ergs/cm^2/\mathring{A}$  units) and take a new difference image. This was done to reduce the white-regions surrounding what otherwise

seems to be bright (black) HII-regions. After convolving most of these disappear, as shown in Fig 3. This

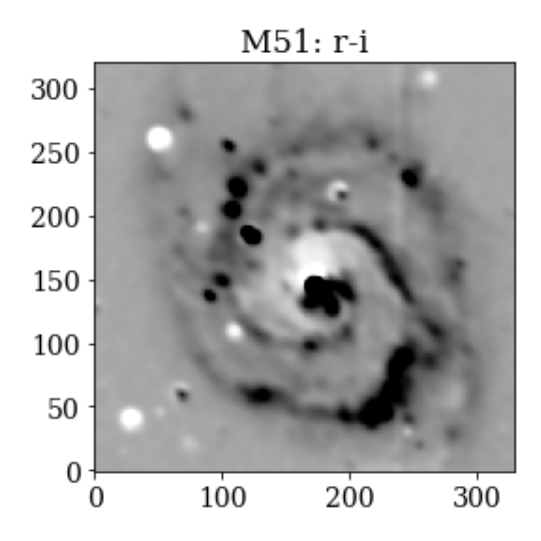


Figure 3. Difference image for M51 taken by subtracting the convolved i-band from the convolved r-band. The spiral arms seem to be host for bright Ha-regions.

image was then exposed to DaoFind and the positions were extracted, shown in Fig. 4.

#### 3.2.2. Method 2 - NGC6946

The identification process was here simplified by having an image in the  $H\alpha$ -filter. For NGC6946 the r image was subtracted from the  $H\alpha$  image after converting both of them to units of  $\mu Jy$ ; the difference image,  $H\alpha$ -r, was then highlighting the regions bright in  $H\alpha$  and the image was then exposed to DaoFind and the result is shown in Fig. 4.

## 3.3. Calculating the Ha luminosity

After matching regions in the difference images with stars in the original r- and i-images for M51 and M81 and in r- and H for NGC6946, shown in Appendix D, the Ha-luminosity in these regions were calculated.

By using the  $f_{\lambda}$ -values for the fluxes we found the Ha flux through

$$F_{Ha} = \left( f_{\lambda,r} - f_{\lambda,i} \frac{\lambda_r^{\beta}}{\lambda_i^{\beta}} \right) \Delta \lambda_r, \tag{4}$$

where  $\Delta \lambda_r = 1125$  Å is the width of the r-filter and  $\beta = -0.5$ , which is the slope of the continuum spectra of the galaxies. This comes from the fact that continuum in galaxies are usually not flat, so we model it through an exponential depending on the wavelength, i.e.,

$$f_{\lambda,cont} = f_{cont,0} \lambda^{\beta}. \tag{5}$$

In turn,  $F_{Ha}$  is derived by using that  $f_{\lambda,r} = f_{cont,0} \lambda_r^{\beta} + \frac{F_{Ha}}{\Delta \lambda_r}$  and  $f_{\lambda,i} = f_{cont,0} \lambda_i^{\beta}$ . Thereafter the luminosity L can be calculated by

$$L_{Ha} = 4\pi d^2 F_{Ha},\tag{6}$$

where d is the distance to the galaxy. By convention a final conversion to log-units is carried out through

$$L_{Ha,log} = \log_{10}(L_{Ha}). \tag{7}$$

The result is shown in Fig. 5.

Thanks to having the  $H\alpha$  the Luminosity could be calculated by combining

$$f_{\lambda,NB} = f_{\lambda,NB} + \frac{F_{Ha}}{\Delta \lambda_{NB}}$$

$$f_{\lambda,BB} = f_{\lambda,BB} + \frac{F_{Ha}}{\Delta \lambda_{BB}}$$
(8)

where  $f_{\lambda,NB}$  and  $f_{\lambda,NB}$  are the narrowband (H-filter) and broadband (r-band) fluxes, and  $f_{cont}$  is the average continuum flux. Solving for  $F_{Ha}$  yields

$$F_{Ha} = \frac{f_{\lambda,BB} - f_{\lambda_NB}}{\frac{1}{\Delta \lambda_{BB}} - \frac{1}{\Delta \lambda_{NB}}},\tag{9}$$

where  $\Delta \lambda_{NB} = 50$  Å and  $\Delta \lambda_{BB} = 1125$  Å are the central wavelengths for the narrowband and broadband respectively. From here, Eq. (6) and (7) could be used as above to calculate the correspoding luminosities. The final result is shown in Fig. 5. In Fig 6 RGB images for the galaxies are produced for M51 and M81 by letting r-i,r and g be RGB respectively; for NGC6946, H-r,r and H are RGB. Thus,  $H\alpha$ -regions will be red.

## 4. ESTIMATING THE ERROR

To estimate what part of the data that is trustworthy an error was calculated from the original backgroundsubtracted images. 2500 random apertures were placed on each galaxy's r-image; all points were placed outside the galaxy-region. As all images had been backgroundsubtracted they all had medians around 0. flux-distributions were therefore gaussian-like centered around 0. After neglecting some of the most positive fluxes (as these would represent actual sources) the standard deviation for these distributions were calculated and were taken as the errors for the fluxes in counts. These errors were then propagated through the calculations in Section 3.3. The errors in luminosity for  $H\alpha$ were multiplied by 5 to get estimations for S/N = 5, and then the logarithm of these values were taken. In Fig. 5 the errors are displayed as vertical lines.

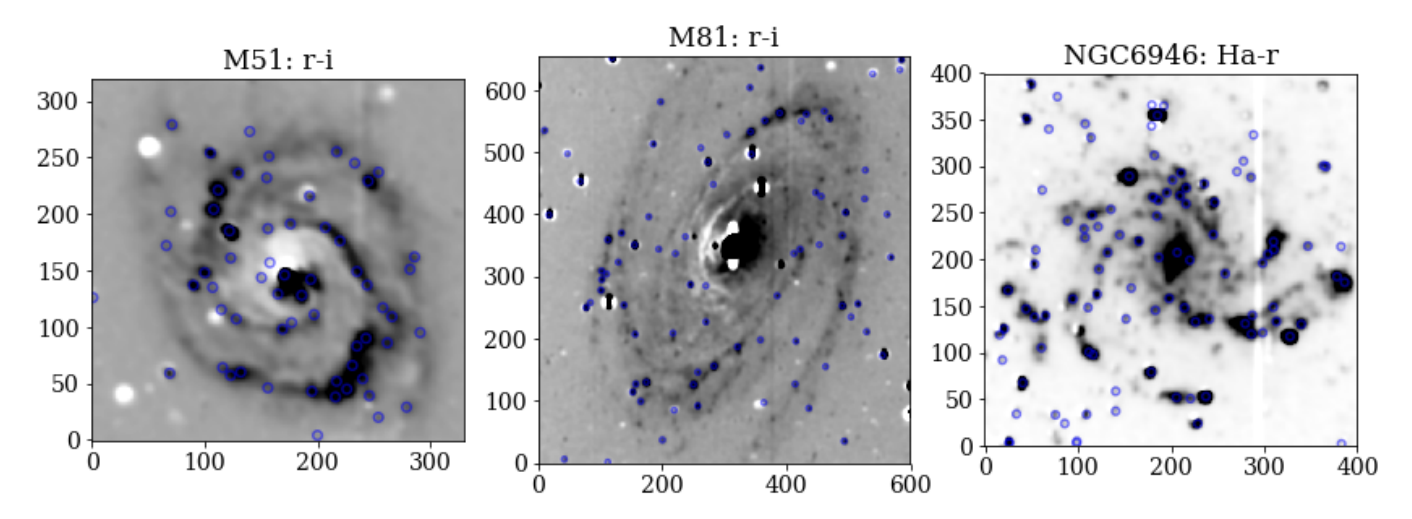


Figure 4. After convolution the i was subtracted from r for M51 and M81, and r was subtracted from  $H\alpha$  for NGC6946. Then DaoFind was used to identify the Ha-regions, seen in the blue circles.

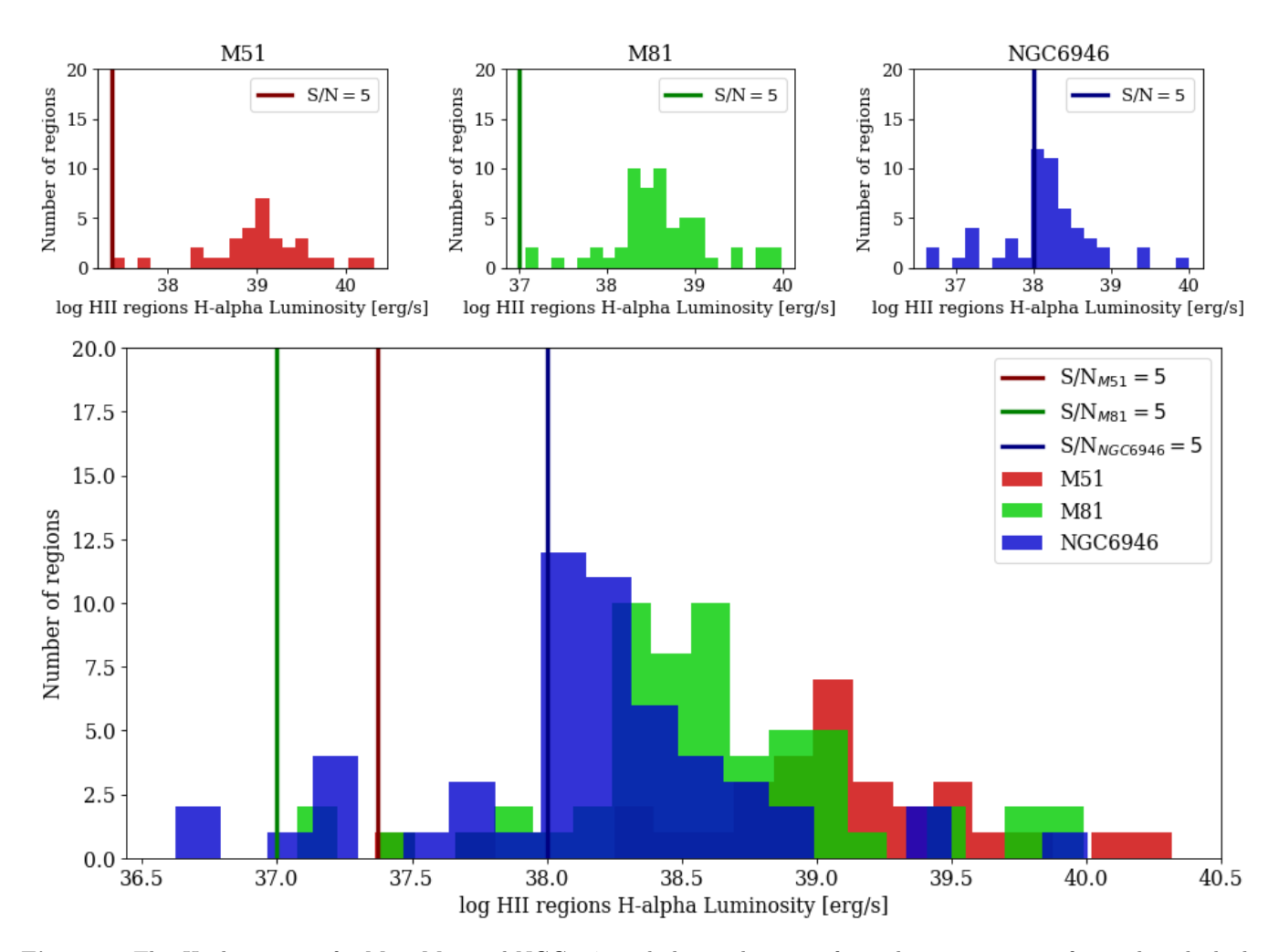


Figure 5. The  $H\alpha$ -luminosity for M51, M81 and NGC6946 including indication of signal-to-noise ratios of 5, under which the data shouldn't be trusted.

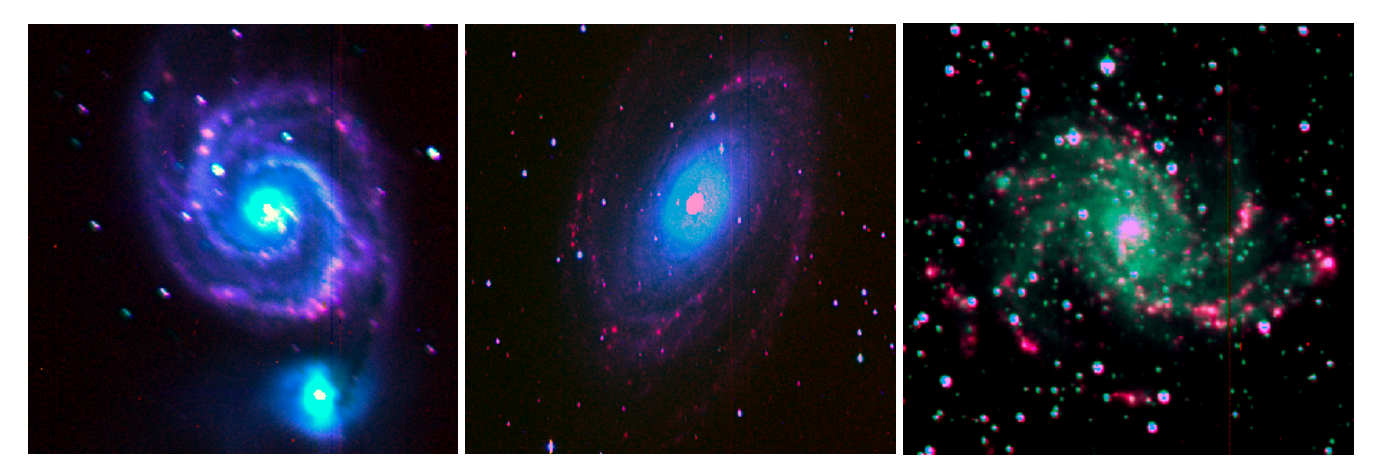


Figure 6. RGB images made for the galaxies M51, M81 and NGC6946.  $H\alpha$ -regions are highlighted by red areas in the images.

#### 5. DISCUSSION

What we see in Fig. 5 are strong indications of star forming regions at the locations displayed in Fig. 4. These so-called HII regions are excellent tracers of star formations since the flux is mainly coming from the recombination of hydrogen, a process which is especially evident when stars are forming.

In Fig. 5 we can see that the luminosities for all galaxies lie between 36 and 40 in log-units, which are reasonable values to obtain when comparing to Miller & Hodge (1994); Lee et al. (2011); García-Benito et al. (2010) for M51,M81 and NGC6946 respectively. However, the values for M51 and M81 seem slightly larger as calculated here compared to Miller & Hodge (1994); Lee et al. (2011), which could be a result of the alternative method used to calculate these methods. So when comparing M51/M81 with NGC6946 we have to bear

in mind that different methods were used to calculate the luminosities; therefore it's hard to with any confidence draw conclusions from M51/M81 seemingly being brighter than NGC6946.

However, as the same method for calculating the luminosities was used for M51 and M81, we here note that the luminosites in M51 seem to be larger. This could be an indication of M51 having more prominent star formation going on. At the same time, however, the number of regions in total seem to be larger in M81. By comparing Bastian et al. (2004) and Kong et al. (2000) as a whole it seems that M51 is a younger galaxy, which however would be hard to determine with the data given here. It might have been possible if  $method\ 2$  would have been applicable on M51/M81, i.e., if data in the  $H\alpha$ -filter would have been obtained.

#### REFERENCES

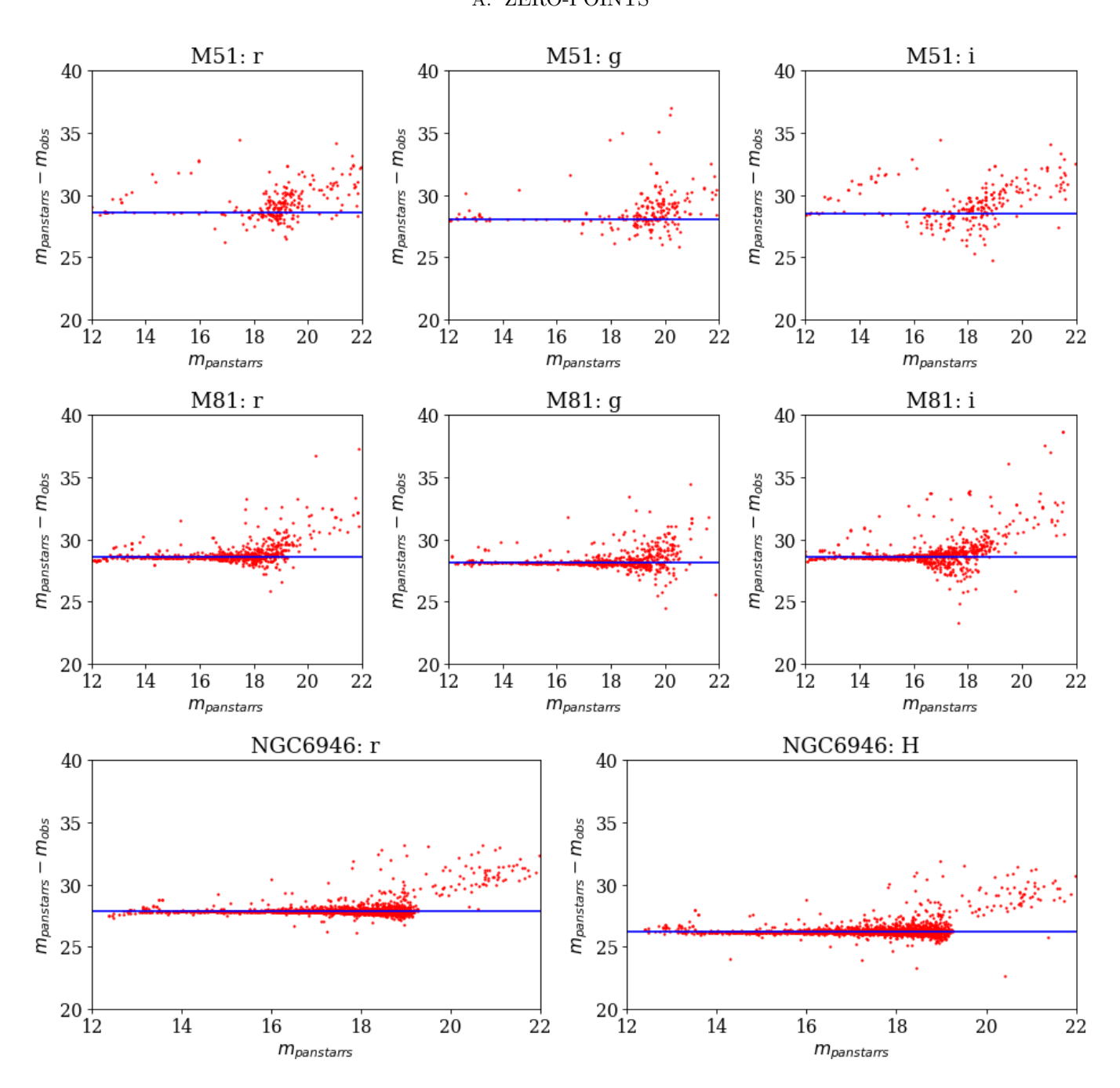
Bastian, N., Gieles, M., Lamers, H. J. G. L. M., Scheepmaker, R. A., & De Grijs, R. 2004, The Star Cluster Population of M51: II. Age distribution and relations among the derived parameters, Tech. rep.

García-Benito, R., Díaz, A., Hägele, G. F., et al. 2010, Mon. Not. R. Astron. Soc, 408, 2234, doi: 10.1111/j.1365-2966.2010.17269.x Kong, X. U., Zhou, X. U., Chen, J., et al. 2000, SPATIALLY RESOLVED SPECTROPHOTOMETRY OF M81 : AGE, METALLICITY, AND REDDENING MAPS, Tech. rep.

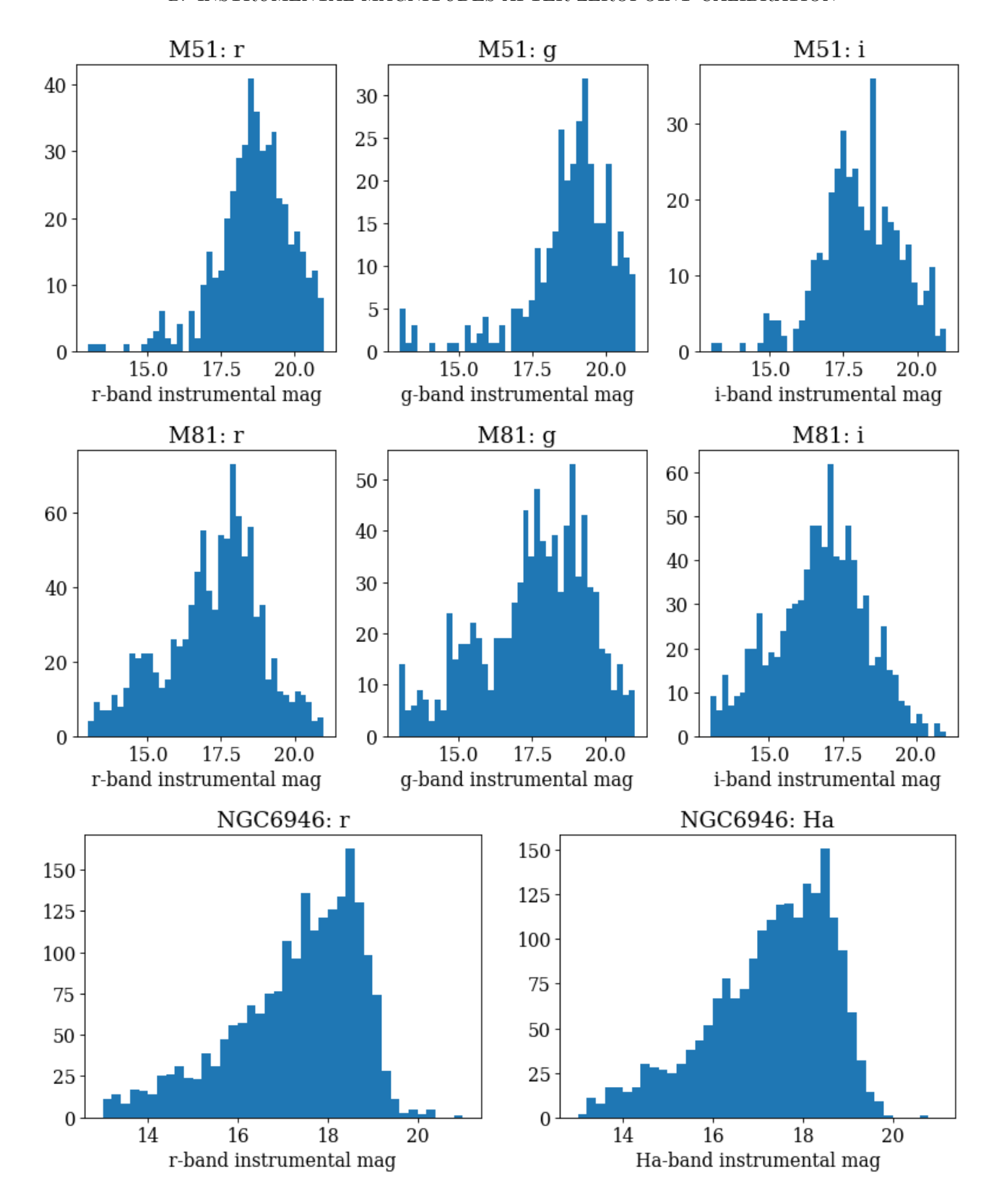
Lee, J. H., Hwang, N., & Lee, M. G. 2011, H II Region Luminosity Function of the Interacting Galaxy M51, Tech. rep. https://arxiv.org/abs/1104.3669v1

Miller, B. W., & Hodge, P. 1994, The Astrophysical Journal. https://arxiv.org/abs/427:656-675

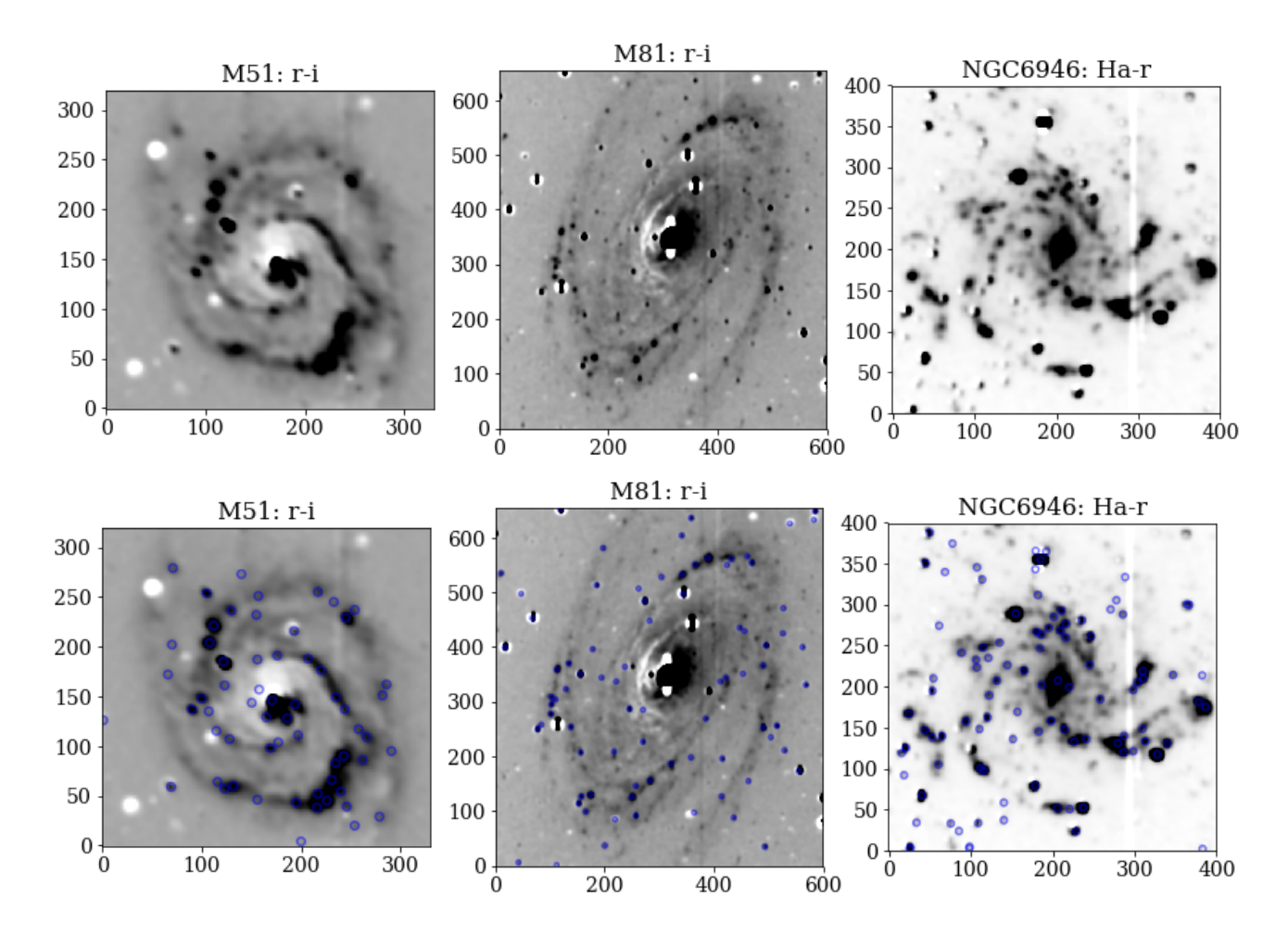
# $\begin{array}{c} \text{APPENDIX} \\ \text{A. ZERO-POINTS} \end{array}$



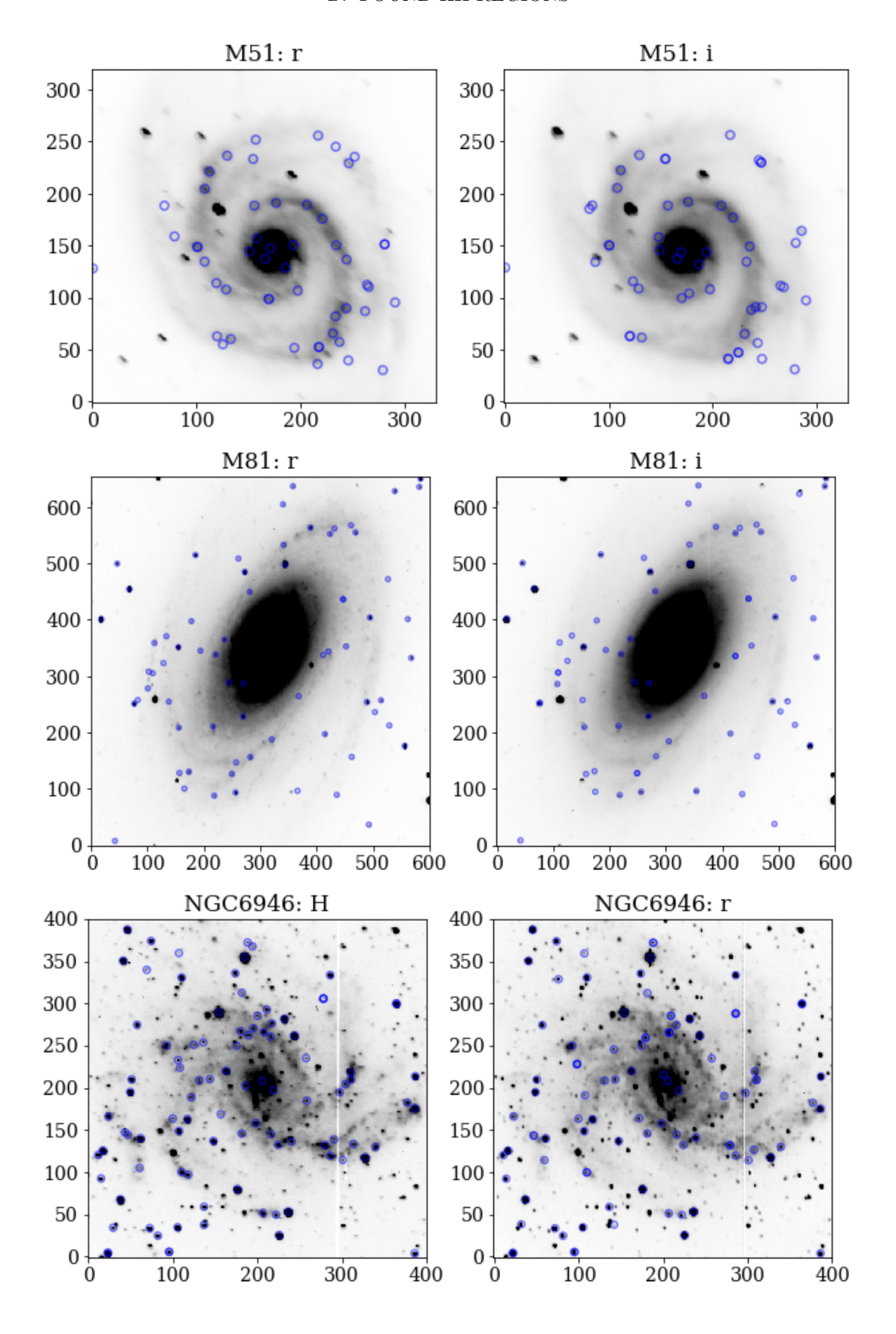
## B. INSTRUMENTAL MAGNITUDES AFTER ZEROPOINT-CALIBRATION



# C. DIFFERENCE IMAGES USED TO IDENTIFY HII-REGIONS



## D. FOUND HII-REGIONS



# E. SELFIE

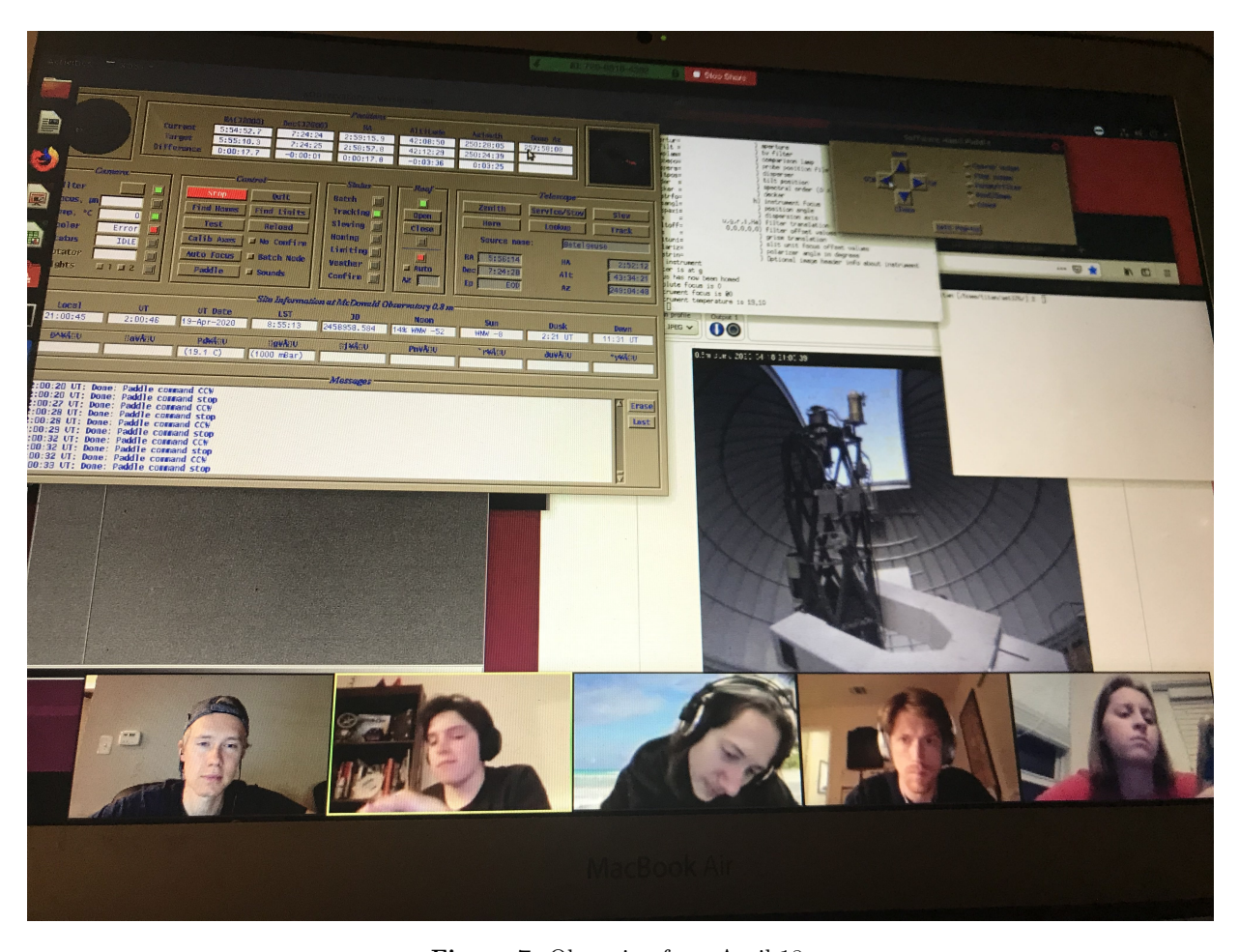


Figure 7. Observing from April 18.

# F. OBSERVATION LOG

Figure 8. Observation Log from April 18.